

Article

Preparation of Highly Active Cu/SiO₂ Catalysts for Furfural to 2-Methylfuran by Ammonia Evaporation Method

Xinxin Fu, Yan Liu, Qiaoyun Liu *, Zhongyi Liu * and Zhikun Peng *

Green Catalysis Center, Henan Institutes of Advanced Technology, College of Chemistry, Zhengzhou University, Zhengzhou 450001, China; fu8545443@163.com (X.F.); liuyan2018@gs.zzu.edu.cn (Y.L.)

* Correspondence: liuqiaoyun@zzu.edu.cn (Q.L.); liuzhongyi@zzu.edu.cn (Z.L.); zhikunpeng@163.com (Z.P.); Tel.: +86-371-67783384 (Z.P.)

Abstract: Biomass plays an important role in the green manufacture of high value-added chemicals. Among them, the conversion of furfural (FFA) into 2-methylfuran (2-MF), catalyzed by a copper-chromium catalyst, is important in its industrial application. However, the use of chromium is limited due to its toxicity and pollution of the environment. In this paper, a Cu/SiO₂ catalyst, prepared by the ammonia evaporation method, shows a better catalytic performance compared with that prepared by the co-precipitation method for the vapor-phase hydrodeoxygenation of FFA. The selectivity of 2-MF is higher than 80% with almost a complete conversion of FFA. Combined with the characterizations, the superiority of the ammonia evaporation method is attributed to the reduction of highly dispersed copper species and the increased Cu⁺/(Cu⁺ + Cu⁰) ratio due to the formation of a large content of copper phyllosilicate during the preparation. Moreover, Cu⁺ sites can act as a weak acid site, which improve the surface acidity of the catalyst and facilitate the formation of 2-MF. This new catalytic system provides a feasible and promising strategy for the industrial preparation of 2-MF from FFA, and effectively utilizes biomass resources to promote the development of biomass industry.



Citation: Fu, X.; Liu, Y.; Liu, Q.; Liu, Z.; Peng, Z. Preparation of Highly Active Cu/SiO₂ Catalysts for Furfural to 2-Methylfuran by Ammonia Evaporation Method. *Catalysts* **2022**, *12*, 276. <https://doi.org/10.3390/catal12030276>

Academic Editors: Maria Luisa Di Gioia, Luisa Margarida Martins and Isidro M. Pastor

Received: 29 January 2022

Accepted: 28 February 2022

Published: 1 March 2022

Publisher's Note: MDPI stays neutral with regard to jurisdictional claims in published maps and institutional affiliations.



Copyright: © 2022 by the authors. Licensee MDPI, Basel, Switzerland. This article is an open access article distributed under the terms and conditions of the Creative Commons Attribution (CC BY) license (<https://creativecommons.org/licenses/by/4.0/>).

Keywords: biomass; 2-methylfuran; Cu/SiO₂; copper phyllosilicate; hydrogenolysis

1. Introduction

Furfural (FFA), an important bio-based platform molecule, has been industrially produced. The catalytic conversion of FFA into high value-added products, such as furfuryl alcohol, 2-methylfuran (2-MF), 2-methyltetrahydrofuran, 3-acetylpropanol and cyclopentanone [1–5], is an important method of biomass utilization. Additionally, 2-MF is an important organic raw material, which can be used to synthesize a series of chemical products such as pesticides and antimalarial drugs. At the same time, 2-MF can also act as a substitute or additive agent of fossil fuels [6,7].

The earliest production of 2-MF was through the oxidation of 1,3-pentadiene from fossils, which is undesirable from a green chemistry perspective [8]. Therefore, the production of green chemicals from biomass conversion has received great attention, which not only limits the mitigation of fossil resources, but effectively utilizes the abundant biomass resources. 2-MF could be obtained from FFA by vapor-phase and liquid-phase hydrogenation [9]. For the liquid-phase method, Pd-, Pt-, Cu-, and/or Ni-based catalysts are commonly used [10–12], which have been limited in their industrial applications due to a low yield of 2-MF and difficult separation [12]. Therefore, vapor-phase hydrogenation has received great attention.

It is reported that Cu has a good hydrogenation ability of C-O bonds, while it does not favor the hydrogenolysis of C-C bonds [13,14], thus showing good catalytic activity in the hydrodeoxygenation of FFA. Copper-chromium catalysts are commonly used in the hydrogenation of aldehydes, ketones or esters [15–19]. Adkins et al. [20] found that the earliest copper-chromium catalyst, Cu₂Cr₂O₅, could be utilized in catalytic hydrogenation. However, industrial manufacture is nowadays limited due to the use of Cr, which is toxic

and pollutive to the environment. In recent years, researchers have paid more attention to developing new green copper-based catalysts to replace Cu/Cr catalysts. Yang et al. [21] reported the yield of 2-MF as 94.5% when using a Cu/ZnO catalyst in FFA conversion. They concluded that the higher catalytic performance was benefited from the high dispersion of copper, surface acidity, and the synergistic effect between Cu⁰ and ZnO. Huang et al. [22] reported a combined yield of 83% from FFA to 2-MF and 2-MTHF using a bimetallic Cu-Pd catalyst with 2-propanol as the hydrogen donor. They concluded that the yield of both products can be improved by adjusting the ratio of the two metals of the bimetallic catalyst, and the synergistic effect of Cu-Pd suppressed side reactions. Moreover, the in situ reduction of metal particles also helped to maintain reactivity. Lobo et al. [23] found that the Fe-containing Cu/SiO₂ catalysts had a higher activity from FFA to 2-MF, and the selectivity of 2-MF was 85%. They found that the addition of Fe increased the dispersion of Cu. Moreover, the partial reduction of Fe species enhanced the rapid hydrogenation of furfuryl alcohol to 2-MF. Park S et al. [24] reported the enhanced hydrodeoxygenation of furfural to 2-MF by a mesoporous Cu/Al₂O₃ catalyst, and the yield of 2-MF was 74%. The special pore structure, improved Cu accessibility, Cu⁰/Cu⁺ synergy and metal-support interaction enhanced activity and stability. Li et al. [25] prepared Cu⁰/Cu₂O·SiO₂ catalysts and found that a hydrogen-reduced copper phyllosilicate sample comprising Cu⁰/Cu₂O·SiO₂ sites with interfaces demonstrated high activities. In conclusion, the preparation method of the Cu/SiO₂ catalyst has greatly affect the electronic structure of Cu and catalytic performance. Therefore, the acid sites, Cu⁰ and Cu⁺, in the catalysts are crucial for FFA to 2-MF.

In this work, we synthesize two catalysts by the ammonia evaporation method and the co-precipitation method, which are denoted as Cu/SiO₂ (AE) and Cu/SiO₂ (CP), respectively. The Cu/SiO₂ (AE) catalyst shows a better catalytic performance for the vapor-phase hydrodeoxygenation of FFA to 2-MF versus the Cu/SiO₂ (CP) catalyst. The high activity of the Cu/SiO₂ (AE) catalyst is realized due to the high dispersion of Cu nanoparticles. In addition, copper phyllosilicate is formed during the preparation process using the ammonia evaporation method, which increases the ratio of Cu⁺/(Cu⁺ + Cu⁰) and strengthens the synergistic effect between Cu⁰ and Cu⁺. Moreover, Cu⁺ can enhance oxophilicity and act as a weak acid site to improve the selectivity of 2-MF [24,26]. In conclusion, the Cu/SiO₂ (AE) catalyst provides a new route for the vapor-phase hydrogenation of FFA to 2-MF and a feasible strategy for the industrialized green synthesis of 2-MF.

2. Results and Discussion

2.1. Characterization of Catalysts

The ICP-AES results show that 20 wt% Cu/SiO₂ catalysts are all close to the theoretical values, and the Cu/SiO₂ (AE) catalyst has a larger specific surface area versus the Cu/SiO₂ (CP) catalyst (Table 1). TEM images of Cu/SiO₂ catalysts are shown in Figure 1. For the calcined Cu/SiO₂ (AE) catalyst (Figure 1a), the typical filandrous morphology of copper phyllosilicate is observed [14,27], while no similar structure is observed for Cu/SiO₂ (CP) catalyst. The Cu/SiO₂ (AE) catalyst after reduction (Figure 1b,c) shows that the filandrous morphology of copper phyllosilicate is eliminated substantially [27] and the copper species are highly dispersed. The average diameter of the Cu/SiO₂ (AE) catalyst is about 3.2 nm. However, the Cu/SiO₂ (CP) catalyst (Figure 1d) shows the aggregation of Cu particles and lower dispersion. The average diameter of Cu/SiO₂ (CP) catalyst is about 5.4 nm, which indicates that the formation of copper phyllosilicate may be beneficial for the dispersion of Cu nanoparticles.

Table 1. Physical and chemical property of Cu/SiO₂ (CP) and Cu/SiO₂ (AE) catalysts.

Catalyst	Cu Loading ^a (wt%)	S _{BET} ^b (m ² ·g ⁻¹)	Pore Volume ^c (nm)	I ₆₇₀ /I ₈₀₀ ^d	X _{Cu⁺} ^e (%)
Cu/SiO ₂ (CP)	24	316.6	5.2	0	22
Cu/SiO ₂ (AE)	22	462.3	6.7	0.128	32

^a Determined by ICP-AES; ^b BET specific surface area; ^c BET pore volume; ^d By integration of the fitted peaks at 670 and 800 cm⁻¹ in the FT-IR spectrum; ^e Peak area ratio, X_{Cu⁺} = Cu⁺/(Cu⁰ + Cu⁺).

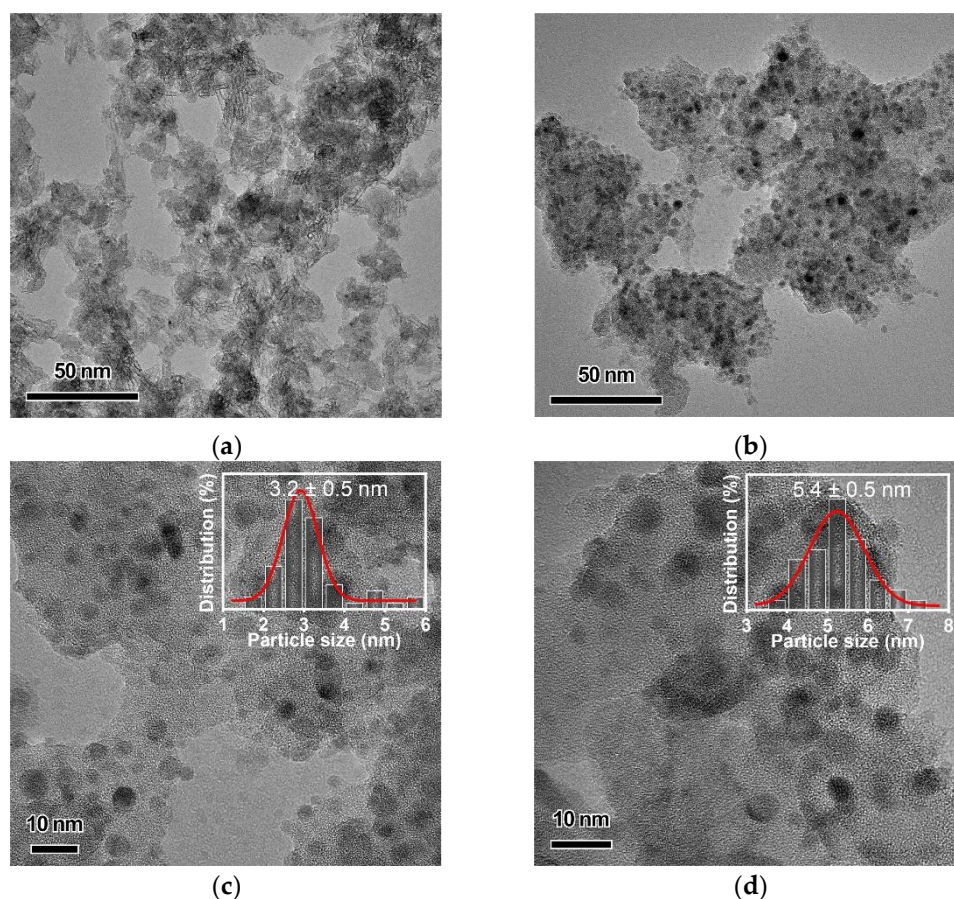


Figure 1. TEM images of (a) Cu/SiO₂ (AE) after calcination; (b,c) Cu/SiO₂ (AE) after reduction; (d) Cu/SiO₂ (CP) after reduction.

FT-IR is further used to determine the existence of copper phyllosilicate. The FT-IR spectra of calcined Cu/SiO₂ catalysts are shown in Figure 2. The absorption bands at 1110, 800 and 470 cm⁻¹ correspond to various vibration modes of the Si-O-Si bonds of amorphous silica [28]. The support of the catalyst prepared by the co-precipitation method and ammonia evaporation method exists in amorphous form. The band at 1640 cm⁻¹ corresponds to the vibrational mode of the -OH of adsorbed water [29,30]. The existence of absorption bands at 1040 cm⁻¹ and 670 cm⁻¹ indicates the existence of the copper phyllosilicate [31]. The absorption band at 1040 cm⁻¹ is ascribed to the vibration mode of Si-O bonds, and the absorption band at 670 cm⁻¹ results from the vibration mode of -OH bond. The relative amount of copper phyllosilicate of the δ_{OH} band at 670 cm⁻¹ and the ν_{Si-O} band of amorphous silica at 800 cm⁻¹ (I₆₇₀/I₈₀₀) [32] are shown in Table 1, which indicates the ratio of copper phyllosilicate. Clearly, the Cu/SiO₂ (AE) catalyst shows more copper phyllosilicate. The formation of copper phyllosilicate indicates the metal-support interaction between copper and the support, which is corroborated by the report that copper can insert into the framework of the silica support and connect to it through

chemical bonds [14]. The existence of this structure is related to the formation of a catalyst with a high dispersion, which is consistent with the results of TEM (Figure 1).

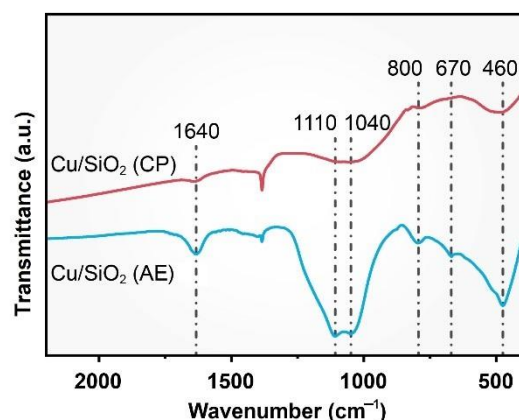


Figure 2. FT-IR spectra of the Cu/SiO₂ (CP) and Cu/SiO₂ (AE) catalysts after calcination.

The XRD patterns of calcined Cu/SiO₂ catalysts are shown in Figure 3a. The two Cu/SiO₂ catalysts have similar diffraction patterns to pure SiO₂. For the Cu/SiO₂ (CP) catalyst, clear CuO diffraction peaks at 35.3° and 38.7° (JCPDS 05-0061) [14,33] are found, which indicate larger CuO nanoparticles. However, no clear CuO diffraction peaks are found for Cu/SiO₂ (AE) catalysts, indicating that no aggregated CuO particles exist. Additionally, the peaks for Cu/SiO₂ (AE) catalysts at 31.0°, 57.0° and 64.1° are assigned to the copper phyllosilicate [14], indicating that copper phyllosilicate is formed after calcination, which is consistent with the results of FT-IR.

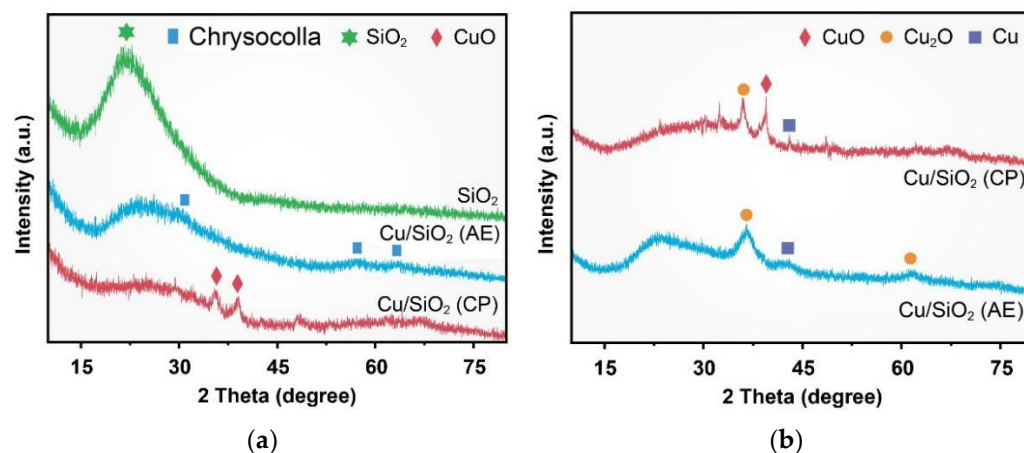


Figure 3. XRD patterns of Cu/SiO₂ (CP) and Cu/SiO₂ (AE) catalysts (a) calcined catalysts; (b) reduced catalysts.

XRD patterns of the reduced Cu/SiO₂ catalysts are shown in Figure 3b. The peak at 38.7° for Cu/SiO₂ (CP) catalysts shows the existence of CuO after reduction, indicating that the catalyst prepared by the co-precipitation method is not fully reduced. Cu/SiO₂ (AE) catalyst has no CuO peak at 38.7°, indicating that CuO is reduced to Cu⁰ and Cu⁺. The disappearance of the peak may be caused by the high catalyst surface area and high metal dispersion. The peak at 43.4° ascribed to Cu is observed for the Cu/SiO₂ (CP) catalyst, indicating larger Cu nanoparticles [34,35]. The weaker peak at 43.4° for Cu/SiO₂ (AE) catalyst may be related to the high dispersion and small size of Cu nanoparticles. The two catalysts show the diffraction peaks at 36.5° and 61.8°, which are attributed to Cu₂O, indicating that Cu⁺ is present in both catalysts.

The H₂-TPR profiles of Cu/SiO₂ catalysts are shown in Figure 4. All samples are calcined in flowing air at 450 °C for 4 h to ensure oxidized Cu species. H₂-TPR shows that the reduction temperature for CuO over the Cu/SiO₂ (CP) catalyst is at 300–420 °C higher than the reduction temperature for the reported Cu-based catalyst [14,16]. This may be due to the reduction of bulk CuO [27]. The Cu/SiO₂ (AE) catalyst shows a reduction peak at 180–230 °C, which is related to the reduction of the high dispersion and small size of CuO according to the literature [14,27,36]. The XRD results of the Cu/SiO₂ (CP) catalyst show that CuO is present after reduction. However, no CuO exists for the Cu/SiO₂ (AE) catalyst after the same reduction process, which is consistent with the H₂-TPR results. TEM results show that the particle sizes of the Cu/SiO₂ (AE) catalyst and Cu/SiO₂ (CP) catalyst are 3.2 nm and 5.4 nm, respectively. The easy reduction of Cu/SiO₂ (AE) may be due to its small particle size and uniform dispersion.

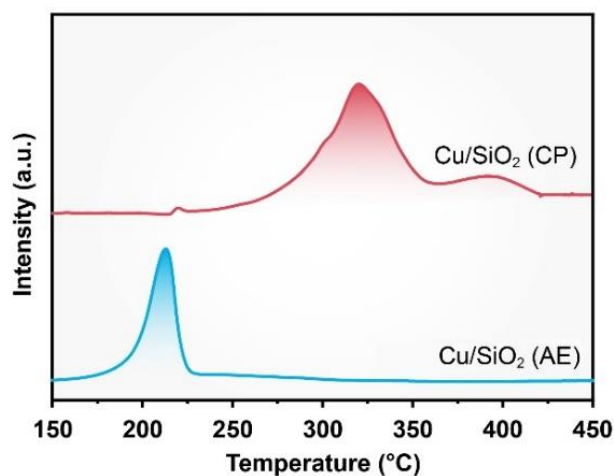


Figure 4. H₂-TPR profiles of the Cu/SiO₂ (CP) and Cu/SiO₂ (AE) catalysts after calcination.

XPS spectra of the Cu/SiO₂ catalysts are shown in Figure 5a. No peak at 940–945 eV is found for the Cu/SiO₂ (AE) catalyst, indicating that Cu²⁺ is totally reduced to Cu⁺ or Cu⁰ [14,16,29], and the two peaks with binding energies at ~932 eV and 952 eV are assigned to the 2P_{3/2} and 2P_{1/2} of Cu⁺ or Cu⁰ [29,37]. The Cu/SiO₂ (CP) catalyst shows a peak at 940–945 eV related to Cu²⁺, indicating the incomplete reduction of CuO. This is consistent with the results of XRD and H₂-TPR. The peak with binding energy at ~935 eV may be related to the 2P_{3/2} of Cu²⁺ [22,27]. The peak with binding energy at 952 eV is assigned to the 2P_{1/2} of Cu⁰ [22]. To further analyze the content of Cu⁺ and Cu⁰, the Cu LMM auger spectra is investigated (Figure 5b). For the Cu/SiO₂ (CP) catalyst, the peak between 910–925 eV is divided into two peaks at 916 eV and 919 eV, which are ascribed to Cu⁺ and Cu⁰ species [26,38]. Accordingly, the Cu/SiO₂ (AE) catalyst shows two peaks for Cu⁺ and Cu⁰ species at 915 eV and 920 eV, respectively [38]. For the Cu/SiO₂ (AE) catalyst, the Cu⁺/(Cu⁰ + Cu⁺) intensity ratio, obtained by fitting the Cu LMM peaks, is 32%, higher than that of Cu/SiO₂ (CP) catalyst (22%) (Table 1) [14].

The NH₃-TPD profiles of Cu/SiO₂ catalysts are shown in Figure 6. For the Cu/SiO₂ (CP) catalyst, the peaks at 90–240 °C and 330–530 °C are attributed to the desorption of NH₃ at weak and strong acid sites. The acid amounts of weak acid and strong acid are 0.03 mmol·g⁻¹ and 0.12 mmol·g⁻¹, respectively. Additionally, the NH₃ desorption peaks at 90–230 °C and 235–370 °C are attributed to the desorption of NH₃ at weak and moderate acid sites for the Cu/SiO₂ (AE) catalyst [26], and the acid amounts of the weak and moderate sites are 0.08 mmol·g⁻¹ and 0.06 mmol·g⁻¹. The report shows that pure CuO and SiO₂ have almost no acidity, and the acid sites of Cu/SiO₂ may be related to the low state copper species, such as Cu⁺ [26,39]. Cu/SiO₂ (AE) catalyst shows more weak acid sites versus the Cu/SiO₂ (CP) catalyst, suggesting that the increased acid sites for the Cu/SiO₂ (AE) catalyst may originate from the higher content of Cu⁺ confirmed by XPS results.

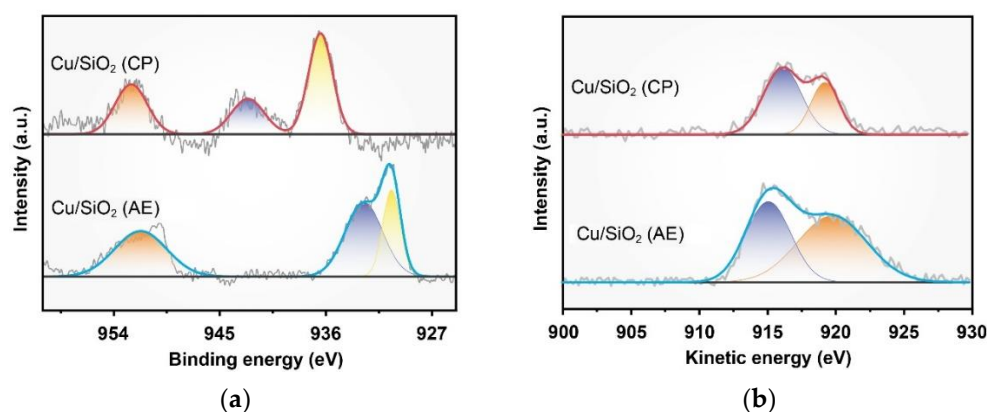


Figure 5. (a) XPS spectra of the Cu/SiO₂ catalysts; (b) Cu LMM Auger spectra of the Cu/SiO₂ catalysts.

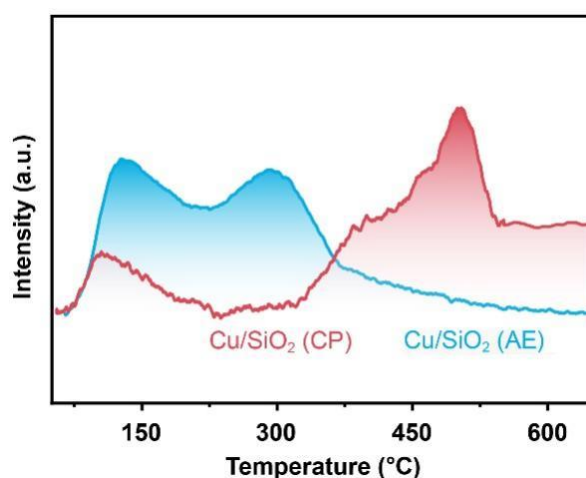


Figure 6. NH₃-TPD profiles of the Cu/SiO₂ (CP) and Cu/SiO₂ (AE) catalysts.

2.2. Catalytic Activity and Stability

The catalytic performance of Cu/SiO₂ catalysts for the vapor-phase hydrogenation of FFA to 2-MF is further studied (Figure 7). The conversion of FFA into 2-MF is achieved through two-step reaction as follows. Firstly, FFA is hydrogenated into furfuryl alcohol (FA), then FA is further converted into 2-MF by the cleavage of C-O bonds through hydrogenolysis (Scheme 1) [25,40]. In this work, the metal loading of Cu is chosen based on the previous work, and two catalysts prepared by different methods are compared [24,26]. Interestingly, the selectivity of 2-MF, up to 86% (Figure 7a), is obtained for the Cu/SiO₂ (AE) catalyst, a good yield obtained so far in the gas hydrogenation of FFA into 2-MF [24,41]. However, only 80% FA and 5% tetrahydrofurfuryl alcohol (THFA) are produced for the Cu/SiO₂ (CP) catalyst. The conversions of FFA over the two catalysts are both close to 100%, indicating that the hydrogenation of FFA is easy and would not be the rate-limiting step. The reaction rates of the Cu/SiO₂ (AE) catalyst and Cu/SiO₂ (CP) catalyst are 10.4 mmol·h⁻¹ and 9.8 mmol·h⁻¹, respectively. The conversion rate of FFA for the Cu/SiO₂ (AE) catalyst is a little higher than that for the Cu/SiO₂ (CP) catalyst, which may benefit from the high dispersion of Cu nanoparticles and the higher reduction degree of CuO. It is interesting that the further conversion of FA is totally different. FA is further hydrogenated into THFA for the Cu/SiO₂ (CP) catalyst by the further hydrogenation of the C=C bond. No FA or THFA is found for the Cu/SiO₂ (AE) catalyst, suggesting that C-O bond hydrogenolysis is preferred rather than the hydrogenation of C=C bond. Park S et al. [24] ascribed the high selectivity and stability of 2-MF over the Cu/Al₂O₃ catalyst to the smaller size of active copper, the acidity, and the synergy between Cu⁰ and Cu⁺. They concluded that Cu⁰ and Cu⁺ were beneficial for activating molecular H₂ on the surface of metallic copper, and Cu⁺

can enhance oxophilicity. Moreover, Li et al. [26] proposed that the high selectivity of the Cu/SiO₂ catalyst to 2-MF was due to the synergistic effect of metal and weak acid sites. They pointed out that weak acid sites could promote the hydrogenolysis of C-O bonds [42]. Combined with the FT-IR and XPS results, the Cu/SiO₂ (AE) catalyst improved the ratio of Cu⁺/(Cu⁺ + Cu⁰) due to the formation of copper phyllosilicate during its preparation. The NH₃-TPD results also confirmed that the Cu/SiO₂ (AE) catalyst shows more weak acid sites, which may be favorable for the formation of 2-MF [26]. Additionally, it is also interesting to find that the carbon balance for Cu/SiO₂ (AE) is satisfying, while that for Cu/SiO₂ (CP) is lower than 90%, which may be caused by the polymerization of FFA or FA over the strong acid sites.

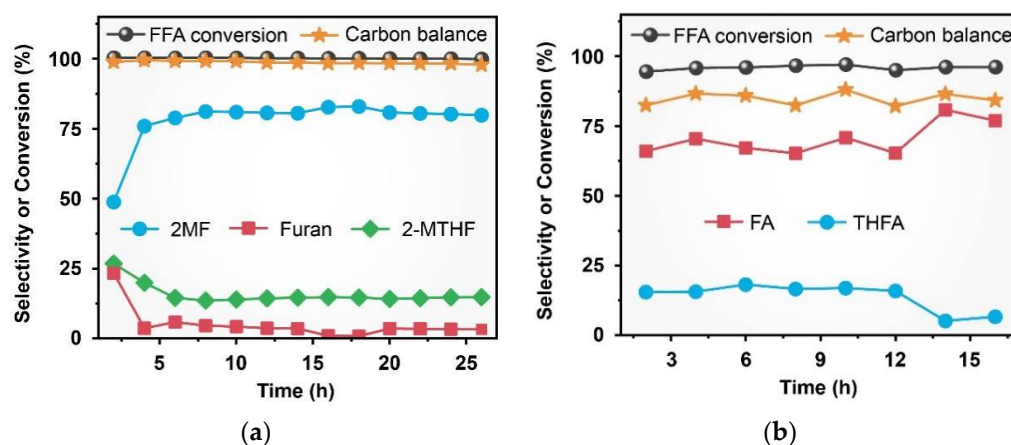
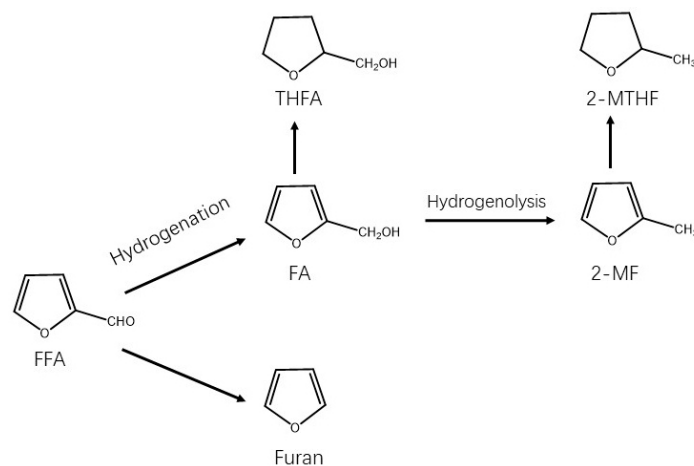


Figure 7. Cu/SiO₂ catalysts for FFA conversion to 2-MF (a) Cu/SiO₂ (AE); (b) Cu/SiO₂ (CP).



Scheme 1. The reaction mechanism for the synthesis of 2-MF.

3. Materials and Methods

3.1. Catalyst Preparation

For the preparation of Cu/SiO₂ catalyst by co-precipitation (Figure 8), 5 g Cu(CH₃COO)₂·H₂O and 20 mL H₂O were mixed and put under ultrasonic for 30 min. Additionally, 16 g Na₂SiO₃·9H₂O was added into 40 mL H₂O to form a solution and kept ultrasonic for 30 min. Then, 4 mL of ammonia water was added to the Cu(CH₃COO)₂·H₂O solution to form a dark blue clear copper ammonia solution. Next the copper ammonia solution was poured into Na₂SiO₃·9H₂O solution to form a mixed solution with PH = 12.8. Then, 8 g CH₃COOH was added dropwise to the mixed solution, and white mist continued to emerge during the process. After stirring for 2 h, the solution was transferred to the hydrothermal reactor and kept at 100 °C for 12 h. Then, the solid was filtered, washed, and dried in a vacuum drying oven at 80 °C for 5 h. The sample was ground and calcined in

flowing air at 450 °C for 4 h to obtain a light green powder, which was denoted as Cu/SiO₂ (CP) with the theoretical loading of Cu at 20 wt%.

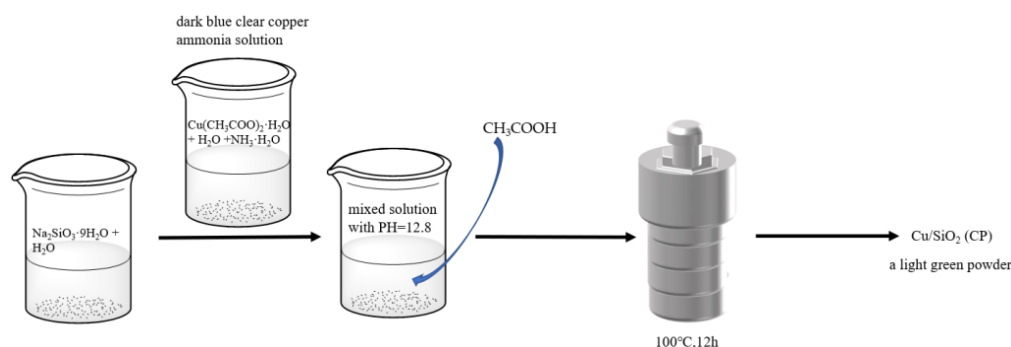


Figure 8. Preparation of Cu/SiO₂ (CP) by co-precipitation.

For the preparation of Cu/SiO₂ catalyst by ammonia evaporation method (Figure 9), 5 g Cu(CH₃COO)₂·H₂O, 2 g of urea and 200 mL H₂O were dissolved and put in a 25 °C water bath. To the mixed solution, 10 g of silica sol (40%) was added and constantly stirred. Then, 10 mL of ammonia water was used to obtain pH = 12. After stirring at 25 °C for 1 h, the temperature was raised to 90 °C and stirred for 1 h. The ammonia was steamed openly to PH = 8, and the solution was a light blue turbid liquid. The solution was transferred to the hydrothermal reactor and kept at 100 °C for 12 h. The sample was filtered, washed, and dried. The sample was ground and calcined in flowing air at 450 °C for 4 h to obtain a light blue powder, which was denoted as Cu/SiO₂ (AE), with the same metal loading as Cu/SiO₂ (CP).

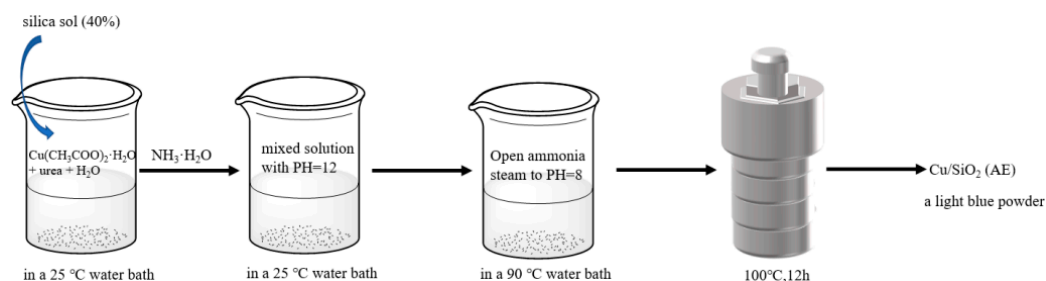


Figure 9. Preparation of Cu/SiO₂ (AE) by ammonia evaporation method.

3.2. Characterization

The X-ray diffraction (XRD) patterns of samples were analyzed on the D8 X-ray diffractometer of Bruker, Germany, with a Cu K α radiation, $\lambda = 1.541 \text{ nm } \text{\AA}$. N₂ adsorption and desorption were performed on the physical adsorption analyzer Micromeritics ASAP 2420 at a temperature of 77 K. The content of copper in the sample was determined by inductively coupled plasma atomic emission spectrometry (ICP-AES). X-ray photoelectron spectroscopy (XPS) and X-ray Auger electron spectroscopy (XAES) of the catalysts were performed on a PHI Quantera SXM spectrometer with Al K $\alpha = 1486.6 \text{ eV}$ as the excitation source, and the binding energy was corrected by setting that of C_{1s} at 284.8 eV. Transmission electron microscopy (TEM) images were obtained using a FEI Tecnai G2 F20 electron microscope operated at 200 kV. Fourier transform infrared (FT-IR) spectroscopy was performed on a Thermo Fisher Nicolet 380. The spectral resolution was 2 cm⁻¹ and 32 scans were recorded for the spectrum. The experiments of temperature-programmed reduction by hydrogen (H₂-TPR) were performed on a Quantachrome Autosorb-IQ gas adsorption analyzer. In the experiment, the sample was calcined in air at 450 °C for 4 h and cooled to room temperature. Then, the TCD signal was collected when the temperature increased to 600 °C at 10 °C min⁻¹ under 10 vol% H₂/Ar. The temperature-programmed desorption

of ammonia (NH_3 -TPD) was performed on a Quantachrome Autosorb-IQ gas adsorption analyzer. The sample was heated from 50 °C to 400 °C at 50 °C·min⁻¹ in He for 30 min and cooled to 100 °C, and 10 vol% NH_3 /He was introduced to achieve saturated adsorption. Then, after purging with He for 1 h to remove NH_3 , which is physically adsorbed, the sample was heated from 100 °C to 700 °C at 10 °C·min⁻¹.

3.3. Catalytic Performance Evaluation

The activity test was conducted on a continuous flow unit equipped with a stainless-steel fixed-bed tubular reactor (Figure 10), where 1 g Cu/SiO_2 catalyst was pressed into tablets and sieved to 20–40 mesh, then loaded into a stainless-steel reactor with an inner diameter of 8 mm. The position of the catalyst bed was fixed with a thin layer of quartz wool to ensure that the catalyst bed was located in the constant temperature section of the stainless-steel reactor. Feed H_2 and the stainless-steel reactor temperature were set to 200 °C, and the vaporizer temperature was set to 260 °C. Furfural was pumped into the vaporizer through a syringe pump for vaporization, and then hydrogen flowed through the vaporizer and was mixed with furfural in the stainless-steel reactor. Among them, the hydrogen space velocity is 400 h⁻¹, and the molar ratio of H_2 and furfural is 10:1. The product is analyzed online by gas chromatography (Agilent GC-7820A) and equipped with a FID detector and HP-INNOWAX column (30 m × 0.32 mm, 0.5 μm).

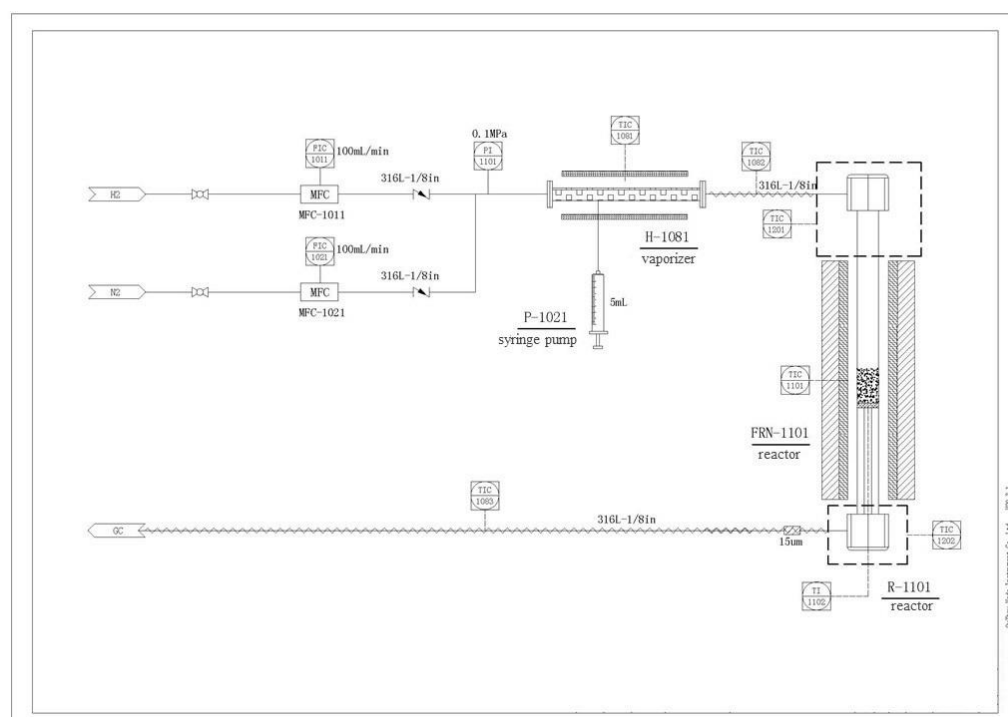


Figure 10. Micro device PID model diagram.

The conversion and selectivity were defined as the following Equations (1) and (2):

$$\text{FFA Conversion (\%)} = \left[\frac{\text{FFA}_{\text{before}} - \text{FFA}_{\text{after}}}{\text{FFA}_{\text{before}}} \right] \times 100\% \quad (1)$$

$$\text{Product Selectivity (\%)} = \left[\frac{\text{Product}_{\text{after}}}{\text{FFA}_{\text{before}} - \text{FFA}_{\text{after}}} \right] \times 100\% \quad (2)$$

4. Conclusions

In this work, Cu/SiO_2 catalysts were prepared for vapor-phase hydrodeoxygenation of FFA to 2-MF by the co-precipitation method (CP) and modified ammonia evaporation method (AE). The Cu/SiO_2 (AE) catalyst shows a superior catalytic performance with a high selectivity of 2-MF versus Cu/SiO_2 (CP) catalyst; 2-MF selectivity still maintains above 80%

within 25 h. The Cu/SiO₂ (AE) catalyst improves the selectivity of 2-MF mainly through the following aspects: (1) The Cu/SiO₂ (AE) catalyst has a high dispersion and small size of copper nanoparticles, due to the formation of the copper phyllosilicate structure. The formation of the copper phyllosilicate structure improves the ratio of Cu⁺/(Cu⁺ + Cu⁰) and enhances the synergy between Cu⁰ and Cu⁺. (2) Cu⁺ sites enhance oxophilicity and act as a weak acid site, which improve the surface acidity of the catalyst, favoring the formation of 2-MF. This work puts forward an efficient strategy and provides a feasible route for the industrial production of 2-MF, which is of great significance in biomass conversion.

Author Contributions: Conceptualization, Z.P. and Z.L.; methodology, Q.L.; software, Y.L.; validation, X.F.; formal analysis, Q.L.; investigation, Y.L.; resources, Z.P.; data curation, X.F.; writing—original draft preparation, X.F.; writing—review and editing, Z.P.; supervision, Z.L. All authors have read and agreed to the published version of the manuscript.

Funding: This research was funded by National Natural Science Foundation of China (No. 21908203, 22108259), Central Plains Science and Technology Innovation Leader Project (No. 241200510006), and Science and Technology Project of Henan Province (212102210192).

Data Availability Statement: Data are contained within the article.

Conflicts of Interest: The authors declare no conflict of interest.

References

1. Hronec, M.; Fulajtarová, K. Selective transformation of furfural to cyclopentanone. *Catal. Commun.* **2012**, *24*, 100–104. [[CrossRef](#)]
2. Jia, P.; Lan, X.; Li, X.; Wang, T. Highly Selective Hydrogenation of Furfural to Cyclopentanone over a NiFe Bimetallic Catalyst in a Methanol/Water Solution with a Solvent Effect. *ACS Sustain. Chem. Eng.* **2019**, *7*, 15221–15229. [[CrossRef](#)]
3. Yan, K.; Wu, G.; Lafleur, T.; Jarvis, C. Production, properties and catalytic hydrogenation of furfural to fuel additives and value-added chemicals. *Renew. Sustain. Energy Rev.* **2014**, *38*, 663–676. [[CrossRef](#)]
4. Schnibpp, L.E.; Geller, H.H.; Korff, R.W. The Preparation of Acetopropyl Alcohol and 1,4-Pentanediol from Methylfuran. *J. Am. Chem. Soc.* **1947**, *69*, 3.
5. Pace, V.; Hoyos, P.; Castoldi, L.; Maria, D.D.P.; Alcantara, A.R. 2-Methyltetrahydrofuran (2-MeTHF): A Biomass-Derived Solvent with Broad Application in Organic Chemistry. *ChemSusChem* **2012**, *5*, 1369–1379. [[CrossRef](#)] [[PubMed](#)]
6. Wang, C.; Xu, H.; Daniel, R.; Ghafourian, A.; Herreros, J.M.; Shuai, S.; Ma, X. Combustion characteristics and emissions of 2-methylfuran compared to 2,5-dimethylfuran, gasoline and ethanol in a DISI engine. *Fuel* **2013**, *103*, 200–211. [[CrossRef](#)]
7. Soledad, Z.M.; Martin, G.; Gustavo, M.; Carlos, Q. Furfural hydrodeoxygenation on iron and platinum catalysts. *Appl. Catal. A-Gen.* **2019**, *587*, 117217.
8. Mariscal, R.; Maireles-Torres, P.; Ojeda, M.; Sádaba, I.; López Granados, M. Furfural: A renewable and versatile platform molecule for the synthesis of chemicals and fuels. *Energy Environ. Sci.* **2016**, *9*, 1144–1189. [[CrossRef](#)]
9. Wang, B.; Li, C.; He, B.; Qi, J.; Liang, C. Highly stable and selective Ru/NiFe₂O₄ catalysts for transfer hydrogenation of biomass-derived furfural to 2-methylfuran. *J. Energy Chem.* **2017**, *26*, 799–807. [[CrossRef](#)]
10. Yu, W.; Tang, Y.; Mo, L.; Chen, P.; Lou, H.; Zheng, X. One-step hydrogenation-esterification of furfural and acetic acid over bifunctional Pd catalysts for bio-oil upgrading. *Bioresour. Technol.* **2011**, *102*, 8241–8246. [[CrossRef](#)]
11. Yan, K.; Chen, A. Selective hydrogenation of furfural and levulinic acid to biofuels on the ecofriendly Cu-Fe catalyst. *Fuel* **2014**, *115*, 101–108. [[CrossRef](#)]
12. Bhogeswararao, S.; Srinivas, D. Catalytic conversion of furfural to industrial chemicals over supported Pt and Pd catalysts. *J. Catal.* **2015**, *327*, 65–77. [[CrossRef](#)]
13. Brands, D.S.; Poels, E.K.; Blik, A. Ester hydrogenolysis over promoted Cu/SiO₂ catalysts. *Appl. Catal. A-Gen.* **1999**, *184*, 279–289. [[CrossRef](#)]
14. Ding, T.; Tian, H.; Liu, J.; Wu, W.; Yu, J. Highly active Cu/SiO₂ catalysts for hydrogenation of diethyl malonate to 1,3-propanediol. *Chin. J. Catal.* **2016**, *37*, 484–493. [[CrossRef](#)]
15. Burnett, L.W.; Johns, I.B.; Holdern, R.F.; Hixon, R.M. Production of 2-Methylfuran by Vapor-Phase Hydrogenation of Furfural. *Ind. Eng. Chem.* **1948**, *40*, 502–505. [[CrossRef](#)]
16. Zhu, S.; Gao, X.; Zhu, Y.; Zhu, Y.; Zheng, H.; Li, Y. Promoting effect of boron oxide on Cu/SiO₂ catalyst for glycerol hydrogenolysis to 1,2-propanediol. *J. Catal.* **2013**, *303*, 70–79. [[CrossRef](#)]
17. Zhang, C.; Wang, D.; Zhu, M.; Yu, F.; Dai, B. Effect of Different Nano-Sized Silica Sols as Supports on the Structure and Properties of Cu/SiO₂ for Hydrogenation of Dimethyl Oxalate. *Catalysts* **2017**, *7*, 75. [[CrossRef](#)]
18. Zhang, C.; Wang, D.; Dai, B. Promotive Effect of Sn²⁺ on Cu⁰/Cu⁺ Ratio and Stability Evolution of Cu/SiO₂ Catalyst in the Hydrogenation of Dimethyl Oxalate. *Catalysts* **2017**, *7*, 122. [[CrossRef](#)]
19. Rao, R.; Dandekar, A.; Baker, R.T.K.; Vannice, M.A. Properties of copper chromite catalysts in hydrogenation reactions. *J. Catal.* **1997**, *171*, 406–419. [[CrossRef](#)]

20. Adkins, H.; Conner, R. The catalytic hydrogenation of organic compounds over copper chromite. *J. Am. Chem. Soc.* **1931**, *53*, 1091–1095. [[CrossRef](#)]
21. Yang, X.; Xiang, X.; Chen, H.; Zheng, H.; Li, Y.W.; Zhu, Y. Efficient Synthesis of Furfuryl Alcohol and 2-Methylfuran from Furfural over Mineral-Derived Cu/ZnO Catalysts. *ChemCatChem* **2017**, *9*, 3023–3030. [[CrossRef](#)]
22. Chang, X.; Liu, A.F.; Cai, B.; Luo, J.Y.; Pan, H.; Huang, Y.B. Catalytic Transfer Hydrogenation of Furfural to 2-Methylfuran and 2-Methyltetrahydrofuran over Bimetallic Copper–Palladium Catalysts. *ChemSusChem* **2016**, *9*, 3330–3337. [[CrossRef](#)]
23. Sheng, H.B.; Lobo, R.F. Iron-Promotion of Silica-Supported Copper Catalysts for Furfural Hydrodeoxygenation. *ChemCatChem* **2016**, *8*, 3402–3408. [[CrossRef](#)]
24. Park, S.; Kannapu, H.P.R.; Jeong, C.; Kim, J.; Suh, Y.W. Highly Active Mesoporous Cu-Al₂O₃ Catalyst for the Hydrodeoxygenation of Furfural to 2-methylfuran. *ChemCatChem* **2020**, *12*, 105–111. [[CrossRef](#)]
25. Li, B.; Li, L.; Sun, H.; Zhao, C. Selective Deoxygenation of Aqueous Furfural to 2-Methylfuran over Cu⁰/Cu₂O·SiO₂ Sites via a Copper Phyllosilicate Precursor without Extraneous Gas. *ACS Sustain. Chem. Eng.* **2018**, *6*, 12096–12103. [[CrossRef](#)]
26. Dong, F.; Zhu, Y.; Zheng, H.; Zhu, Y.; Li, X.; Li, Y. Cr-free Cu-catalysts for the selective hydrogenation of biomass-derived furfural to 2-methylfuran: The synergistic effect of metal and acid sites. *J. Mol. Catal. A Chem.* **2015**, *398*, 140–148. [[CrossRef](#)]
27. Chen, L.; Guo, P.; Qiao, M.; Yan, S.; Li, H.; Shen, W.; Xu, H.; Fan, K. Cu/SiO₂ catalysts prepared by the ammonia-evaporation method: Texture, structure, and catalytic performance in hydrogenation of dimethyl oxalate to ethylene glycol. *J. Catal.* **2008**, *257*, 172–180. [[CrossRef](#)]
28. Huang, Z.; Cui, F.; Kang, H.; Chen, J.; Zhang, X.; Xia, C. Highly dispersed silica-supported copper nanoparticles prepared by precipitation-gel method: A simple but efficient and stable catalyst for glycerol hydrogenolysis. *Chem. Mater.* **2008**, *20*, 5090–5099. [[CrossRef](#)]
29. Natesakhawat, S.; Lekse, J.W.; Baltrus, J.P.; Ohodnicki, P.R.; Howard, B.H.; Deng, X.; Matranga, C. Active Sites and Structure–Activity Relationships of Copper-Based Catalysts for Carbon Dioxide Hydrogenation to Methanol. *ACS Catal.* **2012**, *2*, 1667–1676. [[CrossRef](#)]
30. Chaminand, J.; Djakovitch, L.A.; Gallezot, P.; Marion, P.; Pinel, C.; Rosier, C.C. Glycerol hydrogenolysis on heterogeneous catalysts. *Green Chem.* **2004**, *6*, 359–361. [[CrossRef](#)]
31. Toupance, T.; Kermarec, M.; Lambert, J.F.; Louis, C. Conditions of formation of copper phyllosilicates in silica-supported copper catalysts prepared by selective adsorption. *J. Phys. Chem. B* **2002**, *106*, 2277–2286. [[CrossRef](#)]
32. Toupance, T.; Kermarec, M.; Louis, C. Metal particle size in silica-supported copper catalysts. Influence of the conditions of preparation and of thermal pretreatments. *J. Phys. Chem. B* **2000**, *104*, 965–972. [[CrossRef](#)]
33. Wen, C.; Yin, A.; Cui, Y.; Yang, X.; Dai, W.L.; Fan, K. Enhanced catalytic performance for SiO₂–TiO₂ binary oxide supported Cu-based catalyst in the hydrogenation of dimethyl oxalate. *Appl. Catal. A-Gen.* **2013**, *458*, 82–89. [[CrossRef](#)]
34. Zhao, S.; Yue, H.; Zhao, Y.; Wang, B.; Geng, Y.; Lv, J.; Wang, S.; Gong, J.; Ma, X. Chemoselective synthesis of ethanol via hydrogenation of dimethyl oxalate on Cu/SiO₂: Enhanced stability with boron dopant. *J. Catal.* **2013**, *297*, 142–150. [[CrossRef](#)]
35. Yin, A.; Guo, X.; Dai, W.L.; Fan, K. The Nature of Active Copper Species in Cu-HMS Catalyst for Hydrogenation of Dimethyl Oxalate to Ethylene Glycol: New Insights on the Synergetic Effect between Cu⁰ and Cu⁺. *J. Phys. Chem. C* **2009**, *113*, 11003–11013. [[CrossRef](#)]
36. Zhang, B.; Hui, S.; Zhang, S.; Ji, Y.; Li, W.; Fang, D. Effect of copper loading on texture, structure and catalytic performance of Cu/SiO₂ catalyst for hydrogenation of dimethyl oxalate to ethylene glycol. *J. Nat. Gas Chem.* **2012**, *21*, 563–570. [[CrossRef](#)]
37. He, Z.; Lin, H.; He, P.; Yuan, Y. Effect of boric oxide doping on the stability and activity of a Cu–SiO₂ catalyst for vapor-phase hydrogenation of dimethyl oxalate to ethylene glycol. *J. Catal.* **2011**, *277*, 54–63. [[CrossRef](#)]
38. Wang, D.; Yang, G.; Ma, Q.; Wu, M.; Tan, Y.; Yoneyama, Y.; Tsubaki, N. Confinement Effect of Carbon Nanotubes: Copper Nanoparticles Filled Carbon Nanotubes for Hydrogenation of Methyl Acetate. *ACS Catal.* **2012**, *2*, 1958–1966. [[CrossRef](#)]
39. Gong, J.L.; Yue, H.R.; Zhao, Y.J.; Zhao, S.; Zhao, L.; Lv, J.; Wang, S.P.; Ma, X.B. Synthesis of Ethanol via Syngas on Cu/SiO₂ Catalysts with Balanced Cu⁰–Cu⁺ Sites. *J. Am. Chem. Soc.* **2012**, *134*, 13922–13925. [[CrossRef](#)]
40. Zheng, H.Y.; Zhu, Y.L.; Teng, B.T.; Bai, Z.Q.; Zhang, C.H.; Xiang, H.W.; Li, Y.W. Towards understanding the reaction pathway in vapour phase hydrogenation of furfural to 2-methylfuran. *J. Mol. Catal. A Chem.* **2006**, *246*, 18–23. [[CrossRef](#)]
41. Jiménez-Gómez, C.P.; Cecilia, J.A.; Franco-Duro, F.I.; Pozo, M.; Moreno-Tost, R.; Maireles-Torres, P. Promotion effect of Ce or Zn oxides for improving furfuryl alcohol yield in the furfural hydrogenation using inexpensive Cu-based catalysts. *Mol. Catal.* **2018**, *455*, 121–131. [[CrossRef](#)]
42. Sitthisa, S.; Sooknoi, T.; Ma, Y.; Balbuena, P.B.; Resasco, D.E. Kinetics and mechanism of hydrogenation of furfural on Cu/SiO₂ catalysts. *J. Catal.* **2011**, *277*, 1–13. [[CrossRef](#)]